https://doi.org/10.5194/esd-2020-54
Preprint. Discussion started: 20 July 2020

Earth System Dynamics Discussions

Water transport among the world ocean basins within the water cycle

David García-García[1], Isabel Vigo[1], Mario Trottini[2]

[1]Applied Mathematics Department, University of Alicante, San Vicente del Raspeig, 03690, Spain
[2]Mathematics Department, University of Alicante, San Vicente del Raspeig, 03690, Spain

Correspondence to: David García-García (d.garcia@ua.es)

Abstract. Global water cycle involves water-mass transport on land, atmosphere, ocean, and among them. Quantification of such transport, and especially its time evolution, is essential to identify footprints of the climate change and helps to constrain and improve climatic models. In the ocean, net water-mass transport among the ocean basins is a key, but poorly estimated parameter presently. We propose a new methodology that incorporates the time-variable gravity observations from the GRACE satellite (2003-2016) to estimate the change of water content, and that overcomes some fundamental limitations of existing approaches. We show that the Pacific and Arctic Oceans receive an average of 1916 (95% confidence interval [1812, 2021]) Gt/month (~0.72 ± 0.02 Sv) of excess freshwater from the atmosphere and the continents that gets discharged into the Atlantic and Indian Oceans, where net evaporation minus precipitation returns the water to complete the cycle. This is in contrast to previous GRACE-based studies, where the notion of a seesaw mass exchange between the Pacific and Atlantic/Indian Oceans has been reported. Seasonal climatology as well as the interannual variability of water-mass transport are also reported.

1 Introduction

The water-mass transport (henceforth WT for brevity) in the oceans is a deciding factor of the world climate system. Quantification of such transport, and especially its time evolution, is essential to better understand the climate change. Atlantic Ocean presents notably a deficit of freshwater flux, in contrast to the Pacific Ocean. This produces a salinity asymmetry that explains why deep waters are formed in the North Atlantic and not in the North Pacific (Warren, 1983; Broecker et al., 1985; Rahmstorf, 1996; Emile-Geay et al., 2003; Czaja, 2009). Upper layers of North Atlantic flow northward, while deep waters flow southward, forming the Atlantic Meridional Overturning Circulation (AMOC), which distributes heat within the Earth system and influences temperature and precipitation patterns worldwide (Vellinga and Wood, 2002). While small changes in hydrological cycle may have caused changes in AMOC during the last glaciation that led to abrupt climate changes (Clark et al., 2002), different models project a weakening of the AMOC in the 21st century that would lead to profound climatic and ecological changes in vast regions (Collins et al., 2019). The Antarctic Circumpolar Current (ACC) receives deep water injected by AMOC with excess salinity, which in turn gets transported into the Indian

https://doi.org/10.5194/esd-2020-54
Preprint. Discussion started: 20 July 2020


Earth System Dynamics Discussions

and Pacific Oceans (Warren, 1981). The Indian Ocean returns saltier water, but Pacific and Arctic Oceans return less-salty waters, producing a salinity imbalance in the Atlantic. To restore the balance, freshwater must be transported outside the Atlantic at the rate of 0.13-0.32 Sv through the atmosphere (Zaucker et al., 1994). This WT produces an excess of freshwater in other ocean regions, as in the Pacific and Arctic Oceans, that must discharge out through the ocean.

Meanwhile, conventional observations on the lateral WT of world ocean climatology have been sparse. In fact, measuring such WT in an open ocean region proves difficult as it amounts only to a few tenths Sv, several orders of magnitude smaller than the total ocean water inflow/outflows in such regions. For example, the Pacific is believed to receive regularly an inflow of 157 ± 10 Sv to south of Australia (Ganachaud & Wunsch, 2000), against three outflows: 0.7-1.1 Sv through the Bering Strait (Woodgate et al., 2012), 16 ± 5 Sv through the Indonesian Strait (Ganachaud & Wunsch, 2000), and 140-175 Sv through the Drake Passage (Ganachaud & Wunsch, 2000; Donohue et al., 2016; Colin de Verdière & Ollitrault, 2016; Vigo et al., 2018).

In this work we propose a new methodology devised to estimate the net WT through the boundaries of a given oceanic region. A defining feature of the proposed approach is the use of the time-variable gravity data from the GRACE (Gravity Recovery and Climate Experiment) satellite mission to estimate de change of water content. We apply the methodology, in conjunction with conventional meteorological data of general hydrologic budget schemes, to estimate the time evolution over the period 2003-2016 of the net WT and exchanges among the four major ocean basins – namely Pacific, Atlantic, Indian, and Arctic. We analyse and report our results of the seasonal climatology as well as the interannual variability of WT. Such information, not available previously, would help elucidate the role of the oceans within the water cycle, and constrain ocean models (Warren, 1983; Rahmstorf, 1996; Emile-Geay et al., 2003; de Vries & Weber, 2005; Dijkstra, 2007).

2. Methodology and Data

The general hydrologic budget equation states that, at any continental location and any moment in time, the change of water content dW equals the precipitation P minus evapotranspiration E (as vertical transport) minus the net runoff R (as horizontal transport):

$$dW = P - E - R \qquad \text{for land.} \qquad (1)$$

Under the conservation of water mass, the global net $P-E$ over ocean is negative [e.g., Hartmann, 1994]. That amount of water gets transported to land through atmosphere and returns to the ocean as R completing the water cycle. The general R for a river basin connected to the ocean consists of river runoff, land ice melting, and submarine groundwater discharge to ocean.

https://doi.org/10.5194/esd-2020-54
Preprint. Discussion started: 20 July 2020


Earth System Dynamics Discussions

For an ocean region, R represents the inflow from adjacent land regions plus an extra additive term, call it N, accounting for water exchange between neighbouring ocean regions through boundaries, as (positive) inflow or (negative) outflow:

$$dW = P - E + R + N \qquad \text{for ocean.} \qquad (2)$$

The ocean water flux N is the target quantity that we shall solve for as a residual in Equation 2, which up till now has been infeasible to estimate directly [Rodell et al., 2015]. Note that N represents the integrated WT over the total-column depth of ocean, including deep-water flows. This is a strength of the GRACE observation for the oceans, compared to in-situ or other remote-sensing measurements typically targeting only the surface layer.

Our targeted four ocean basins are largely separated geographically with designated continental boundaries and restricted water throughways. The land is divided into their associated drainages according to the global continental runoff pathways scheme of Oki & Sud (1998). There are no direct water exchanges in the form of R among land drainages (see Figure 1). The WT component R is estimated through Equation (1) over each continental region, then input to Equation (2) to estimate N in the associated ocean basins.

The P–E data we use are adopted from the ERA5 reanalysis [Hersbach, 2018], which assimilates observations into general-circulation modelling provided by the European Centre for Medium-Range Weather Forecasts (ECMWF). They are given at 0.25º latitude/longitude regular grids and monthly (and hourly) intervals for global coverage of both continents and oceans. In order to match the spatial resolution of the above-mentioned continental runoff pathways data, we homogenise the grid to 1ºx1º by averaging the corresponding 0.25º grid points.

The critical knowledge needed in Equations (1) and (2), now obtainable from GRACE monthly data, is dW (Tapley et al., 2004, 2019), the month-to-month difference of the stored water. Note that the GRACE mass variability pertains to WT directly, as opposed to, for example, altimetric sea level measurements that also contain non-WT, steric effects. We use the GRACE "mascon" (mass concentration) solutions that have already been converted into surficial mass from the original time-variable gravity observations (in our case the GRACE RL06 mascon dataset provided by the Center of Space Research of University of Texas; see Save et al., 2016, Save, 2019). The non-surficial gravity change due to the glacial isostatic adjustment (GIA) has been removed to the extent of the ICE6G-D model (Peltier et al., 2018). Any other non-surficial effect such as long-term tectonics do masquerade as mascons (Chao, 2016) but are here ignored; so are the non-climatic sources such as the rare, local earthquake events. As is a common practice, the C_{20} Stokes coefficient is replaced with the solution from Satellite Laser Ranging (Cheng & Ries, 2017). GRACE is not sensitive to the geocenter variations, and its degree-1

https://doi.org/10.5194/esd-2020-54
Preprint. Discussion started: 20 July 2020


Earth System Dynamics Discussions

Stokes coefficients are set to zero. We had tried adding to GRACE data an estimate of geocenter variations due to modelled water-mass variability (Swenson et al., 2008), and our reported results would change less than 1%. On the other hand, we do add back the GAD product, the oceanic effects on gravity change according to the operational numerical weather prediction (NWP) model from ECMWF and to an unconstrained simulation with the global ocean general circulation model MPIOM, respectively (Dobslaw et al., 2017). The GAD had beforehand been removed from the processing of the GRACE data for de-aliasing purposes, now added back so that we recover the "true" ocean mass variability. Data are provided on a 0.25º regular grid; we reduce it to 1º regular grids, still finer than the spatial resolution of GRACE (~300 km), to match the spatial resolution of the continental drainage basin data as above.

GRACE's degree-0 Stokes coefficients ΔC_{00} is set identically to zero on the recognition that the total mass is constant. The GAD product adjustment is performed by the GRACE project in such a way that the atmospheric and dynamic oceanic mass changes are removed beforehand. After that, the GRACE ΔC_{00} are still set to zero even though they should match the opposite of the removed signals by GAD. To restore the lost degree-0 signal, the GAD product must be added back to GRACE with averaged ocean signal set to zero, and then, the ΔC_{00} from an atmospheric model must be subtracted from GRACE data. Doing so, the GRACE data will account for the global exchange of water-mass between the Earth surface and atmosphere. Such correction has recently proved to improve the agreement between the GRACE global ocean mass change and non-steric sea level variation estimates from altimetry and ARGO data (Chen et al., 2019). Looking for consistency between the GRACE and ERA5 datasets, we use ΔC_{00} from $P - E$ to restore degree-0 signal in dW. This ΔC_{00} accounts for uniform mass variations in the global surface equivalent to a global averaged signal for $P-E$, at 188 Gt/month (95% confidence interval CI_{95}=[136, 243], see below). As global $-(P-E)$ represents the variability of global total-column water (TCW), it should match the time derivative of the global TCW. However, the average rate of change of the global TWC in ERA5 is 1.5 Gt/month (CI_{95}=[−9.2, 12.7]), although in the range of previously reported values of [−0.9, 4.3] Gt/month [Nilsson & Elgered, 2008] departs far from the global $-(P-E)$ value. This reveals some internal inconsistency within the ERA5 dataset. However, while artificially increasing the dW estimate, the excessive value of $P-E$ does not affect the WT components R and N estimated from Equations (1) and (2), since the degree-0 signal vanishes due to the residual estimate between dW and $P-E$. In fact, adding ΔC_{00} from $P-E$ to GRACE is numerically equivalent to setting $P-E$ ΔC_{00} to zero as far as Equations (1) and (2) are concerned.

The reported 95% confidence intervals and the correlation coefficients are evaluated using the stationary bootstrap scheme of Politis and Romano (1994) (with optimal block length selected according to Patton et al., 2009), and the quantile method. The number of bootstrap replications is set to 2000. In general, half length of the confidence interval can be very well approximated by twice the standard deviation of the sample mean estimated from the bootstrap replications. Prior to applying the bootstrap, least-squares estimated linear/quadratic trend and sinusoid with the most relevant frequencies are

https://doi.org/10.5194/esd-2020-54
Preprint. Discussion started: 20 July 2020


Earth System Dynamics Discussions

removed to meet the stationarity conditions of the method and to avoid spurious correlation. In particular, for the WT *N* component we proceed as follows: (i) a model with linear, annual, and semiannual signals is fitted to the data and subtracted; (ii) 2000 bootstrap samples of the residuals are generated; (iii) these are added back to the fitted model to obtain 2000 bootstrap samples of the original time series. These samples are then used to obtain point estimates of the mean fluxes, the annual amplitudes and phases, and the corresponding quantile-based 95% confidence intervals. In order to study the robustness of the results with respect to the model choice, the analysis is rerun using 11 alternative models obtained considering different forms for the trend component (quadratic or constant) and including higher frequencies in the harmonic regression (up to 5). The results are robust. The relative difference with respect to the reported values is smaller than 1.2% for point estimates and smaller than 3.3% for the extremes of the 95% confidence intervals.

3. Results

The various WT components of the Pacific and its associated land drainage regions are shown in Figure 2 in units of Gt/month (1 Sv ≈ 2600 Gt/month, 1 Gt = 10^{12} kg). The same analysis is applied to the rest of the ocean basins, i.e. the AIA oceans individually and collectively, with its associated land drainages (see Figure 1).

3.1 Mean fluxes

Averaged over the studied 14 years, the Pacific loses water through the atmospheric $P-E$ at the average rate of 142 Gt/month (CI_{95}=[48, 243]), which is greatly over-compensated by inflow R from land of 1403 Gt/month (CI_{95}=[1370, 1436]). From this surplus, a minor (if any) amount of 67 Gt/month (CI_{95}=[25, 108]) stays (and accumulates) in the Pacific, while 1194 Gt/month (CI_{95}=[1096,1291]) is transported horizontally to the "non-Pacific" Atlantic/Indian/Artic (AIA) oceans, which will be called the "Pacific outflow" hereafter.

In the AIA Oceans, the situation is found to be markedly distinct, given the fact that the AIA oceans together have surface area comparable to the Pacific (177×10^6 m^2). The AIA oceans collectively lose 3484 Gt/month (CI_{95}=[3406, 3560]) through the atmospheric $P-E$, that is ~25 times more than does the Pacific. This water deficit is only ~68% compensated by land R inflow of 2378 Gt/month (CI_{95}=[2337, 2419]). With the nominal minor amount of water accumulation at 87 Gt/month (CI_{95}=[44, 130]), the AIA oceans thus presents an average inflow of 1194 Gt/month (CI_{95}=[1102, 1284]) from the Pacific, which will be called the "AIA inflow".

As expected from the overall conservation of water mass inherent in our methodology, the estimated Pacific outflow and AIA inflow match (Figure 3). It is worth mentioning that a difference of 188 Gt/month would exist between the two mean flux values if the degree-0 correction were not applied.

https://doi.org/10.5194/esd-2020-54
Preprint. Discussion started: 20 July 2020


Earth System Dynamics Discussions

Corresponding analyses have been performed for the Atlantic, Indian, and Arctic Oceans separately. The time evolution of the WT components in Eqs. 1 and 2 are shown in Figure 4. On average, the Atlantic receives 926 Gt/month (CI_{95}=[876, 980]; or 0.34 Sv) of salty water, and loses 879 Gt/month (CI_{95}=[828, 930]); a freshwater flux of 0.34 Sv by $P-E+R$, which increases the near-surface salt concentration, enables water to sink in North Atlantic producing deep water. These values are close to the 0.13-0.32 Sv estimated from ocean models, as needed to keep salinity balance in the Atlantic Ocean (Zaucker et al., 1994). Similarly, the Indian Ocean loses 957 Gt/month (CI_{95}=[894, 1022]) of freshwater that is restored by 991 Gt/month (CI_{95}=[907, 1073]) of salty water. The freshwater ($P-E+R$) lost by the Atlantic and Indian Oceans goes to the Pacific (1261 Gt/month, CI_{95}=[1171, 1347]) and Arctic (730 Gt/month, CI_{95}=[712, 747]) Oceans, which return 1194 (CI_{95}=[1096, 1291]) and 723 (CI_{95}=[708, 739]) Gt/month of salty water through the ocean, respectively. Then, the Pacific presents a surplus of freshwater that reduces near-surface salt concentration, which prevents the formation of deep water. Together, the Pacific and Arctic Oceans supply 1917 Gt/month (CI_{95}=[1812, 2021]) of water to the Atlantic and Indian Oceans, where it is reincorporated into the water cycle via net $E-P$.

3.2 Annual climatology

The WT climatology of the N component is estimated in two ways: (1) averaging the 14 N values for each months of the year (Figure 5a); and (2) fitting a linear trend plus annual and semiannual components model as described in Section 2. Annual amplitudes and phases are plotted in Figure 5b and reported, with corresponding 95% quantile-based confidence intervals, in Table 1.

The Pacific and Arctic Oceans show an overall outflow throughout the year, unlike the Atlantic and Indian Oceans, which show an inflow for every month. The Pacific outflow shows a prominent seasonal undulation peaked around August 3 and a peak-to-peak WT variation of ~2000 Gt/month from boreal summer to November, when a near-zero minimum occurs. The Arctic Ocean show half of the Pacific variability and a less pronounced seasonal undulation. A minimum outflow of ~320 Gt/month is reached in March and April, and a maximum ~1300 Gt/month in July. Together, the Pacific and Arctic Oceans send ~3000 Gt/month of seawater to the Atlantic and Indian Oceans during boreal summer, and a minimum amount five times lower, around 600 Gt/month, in November. The annual maximum is reached on August 8th. The Atlantic/Arctic inflow shows a specular behaviour. Separately, the Atlantic and Indian inflows show a similar peak-to-peak variation of ~2000 Gt/month, reaching the maxima in August and May, respectively. The Indian maximum seems to be related to a local maximum of the Pacific outflow. The annual maxima of net WT of the four basins are reached between August 3rd and September 9th , although the annual signals of the Pacific and Indian Oceans almost triple those from Arctic and Atlantic Oceans (Table 1 and Figure 5b).

https://doi.org/10.5194/esd-2020-54
Preprint. Discussion started: 20 July 2020


Earth System Dynamics Discussions Open Access EGU

3.3 Interannual variability

Interannually, the Pacific outflow shows remarkable variability, mainly produced by P on the continents, which is inherited by R, and $P-E$ in the oceans (Figure 2). For example, the Pacific outflow shows a maximum around 1372 Gt/month in 2009 that matches with a $P-E$ maximum in the Pacific, $P-E$ minimum in the AIA oceans, and P minima in the continental basins draining to both Pacific and AIA oceans. The opposite behaviour, that is a minimum around 939 Gt/month is observed in 2010. The difference, 433 Gt/month, is comparable to the discharge of Amazon (Lorentz et al., 2014). In the tropical Pacific, the El Niño/Southern Oscillation (ENSO) is the strong recurring climate pattern involving changes in the temperature of seawater and air pressure in the tropical Pacific Ocean. The ENSO had a mild El Niño phase in 2009 followed by a strong La Niña phase in 2010, that may be related to the interannual variability of the Pacific outflow. To elucidate this, we conduct a correlation study of the interannual Pacific outflow with respect to the major climate oscillations in the Earth's atmosphere-ocean: ENSO, Atlantic Multi-decadal Oscillation (AMO), Antarctic Oscillation (AAO), and Arctic Oscillation (AO). The climatic oscillation is represented by monthly time series of its indices, which are non-dimensional functions of time derived from relevant meteorological observations; their values indicate the polarity and strength of the oscillation at a given epoch. The ENSO oscillations are measured here with the Southern Oscillation Index (SOI), which represents the sea level pressure differences between Tahiti and Darwin, Australia. The AMO is a coherent mode of natural variability based upon the average anomalies of sea surface temperatures, with AMO Index to reflect the non-secular multi-decadal sea surface temperature pattern variability in the North Atlantic basin. The AAO describes the intensity of westerly wind belt surrounding the Antarctic, quantified by the AAO Index, which is the leading principal component of the 700 hPa atmospheric geopotential height anomalies poleward of 20°S. The AO is to be interpreted as the surface signature of modulations in the strength of the polar vortex aloft the Arctic, while the AO Index is constructed by projecting the 1000 hPa height anomalies poleward of 20°N. Figure 6 show all indices with amplitudes normalized to one standard deviation, as well as the de-trend, de-season, standard deviation normalized Pacific outflow. The correlation analysis between the Pacific outflow and the SOI shows no overall correlation during the whole period, meaning that the influence of ENSO on the Pacific outflow may be restricted to the strong phases of ENSO as in 2009 and 2010. A similar lack of correlation is observed with respect to the AMO, AAO, and AO.

4. Discussion and Conclusions.

In this work we present a new methodology that combines GRACE data with the general hydrologic budget equation to estimate the horizontal water-mass convergence/divergence for any oceanic region. We have assumed that the gravity changes are produced by mass changes on the Earth surface, such as in the oceans, so that the mascon solution is physically meaningful (Chao, 2016). Any mis-modelling of the ocean basin "container" volume change due to GIA and other non-

https://doi.org/10.5194/esd-2020-54
Preprint. Discussion started: 20 July 2020


Earth System Dynamics Discussions

surficial changes would masquerade as WT variations. However, they are not critical as far as our non-secular analysis is concerned.

We use the proposed methodology to estimate the net WT and exchanges among the Pacific, Atlantic, Indian, and Arctic Oceans, for the period of 2003 – 2016. Our main finding is that the Pacific and Arctic Oceans, while replenished with precipitation and land runoff, are nearly continuously losing water to the Atlantic and Indian Oceans. In particular, the WT climatology is such that the Pacific Ocean loses water at a rate from near zero to up to the peak of 2000 Gt/month during the boreal summer, which coincides with the maximum of the global atmosphere water content. On top of the climatology, the interannual Pacific water loss varies significantly between ~950 to ~1450 Gt/month annual means during the studied period, but seemingly uncorrelated with ENSO.

The results presented here are consistent with the well-known salinity asymmetry between the Pacific and Atlantic Oceans (Reid, 1953; Warren, 1983; Broecker et al., 1985; Zaucker et al., 1994; Rahmstorf, 1996; Emile-Geay et al., 2003; Lagerloef et al., 2008; Czaja, 2009; Reul, 2014). However, they are in contrast to previous GRACE-based studies where a simple seesaw WT between the Pacific and the Atlantic/Indian oceans was reported [Chambers & Willis, 2009; Wouters et al., 2014]. In those studies, the $P-E+R$ term in Equation 2 in both Pacific and Atlantic/Indian Oceans was approximated by that from the global ocean mean. However, the mean freshwater flux in the Pacific (1261 Gt/month) quite mis-matches that in the Atlantic/Indian Oceans (−1837 Gt/month), meaning that the approximation was quite poor and hence the N term was not properly estimated in these studies (see Supplementary Materials for further discussion).

Differences in freshwater fluxes between the Pacific and Atlantic Oceans produce salinity contrasts, and in turn contrasts on deep water formation. Nevertheless, there are other factors influencing these contrasts such as the narrower extent of the Atlantic (de Boer et al., 2008; Jones & Cessi, 2017), the meridional span of the African and American continents (Nilsson et al., 2013; Cessi & Jones, 2017), and the salty WT from the Indian Ocean to the Atlantic (Gordon, 1986; Marsh et al., 2007). AMOC is also influenced by WT through Bering Strait (Reason & Power, 1994; Goosse et al., 1997; Wadley & Bigg, 2002), and by surface processes of temperature, precipitation and evaporation at low-latitudes of Pacific and Indian Oceans (Newsom & Thompson, 2018). The relative importance among the multiple drivers influencing the AMOC is an open problem (Ferreira, 2018). The net WT estimated here provides information for differences between oceanic inflows and outflows, which can be useful to elucidate on this problem.

Net WT in the open oceans can alternatively be estimated using global ocean models, which simulates observational data based on physical principles. However, these models are not necessarily sensitive to the WT specifically given the data types, and the geography and topography resolutions involved in the models. Knowledge about three-dimensional global

https://doi.org/10.5194/esd-2020-54
Preprint. Discussion started: 20 July 2020

Earth System Dynamics Discussions

ocean circulation could also elucidate on the net WT. However, the small ratio between the net and the total WT hinders the estimation of the former from the latter.

We have applied our WT estimation scheme to the four major ocean basins. The methodology can of course be applied to any extensive ocean region of interest as long as it is much larger than the GRACE resolution. The findings reported here will be useful for a better understanding of the global climate system in terms of its climatology and spatio-temporal variations.

Appendix: Apparent net mass exchange between Pacific and Atlantic/Indian oceans

We shall here that the net water mass exchange between the Pacific and Atlantic/Indian Oceans reported by Chambers and Willis (2009) was a mathematical artefact. Their Equation (2) approximated the freshwater flux, i.e. $P-E+R$, of the Pacific (Pcf) and Atlantic/Indian (AI) oceans by the global ocean (GO) mean. However, from Figures 2 and 4 we get very different $(P-E+R)_{Pcf}$=1261 and $(P-E+R)_{AI}$=−1837 Gt/month, meaning that the approximation in Chambers and Willis (2009) and hence their resultant estimates of WT are rather poor. In addition, under their approximation an apparent net mass exchange will always arise, since

$$(P-E+R)_{GO} = \sum_{x \in GO} \frac{(P-E+R)_x \cdot Area(x)}{Area(GO)} =$$
$$= \sum_{x \in Pcf} \frac{(P-E+R)_x \cdot Area(x)}{Area(GO)} + \sum_{x \in AI} \frac{(P-E+R)_x \cdot Area(x)}{Area(GO)} =$$
$$= \sum_{x \in Pcf} \frac{(P-E+R)_x \cdot Area(x)}{Area(Pcf)} \cdot \frac{Area(Pcf)}{Area(GO)} + \sum_{x \in Atl/Indian} \frac{(P-E+R)_x \cdot Area(x)}{Area(AI)} \cdot \frac{Area(AI)}{Area(GO)} \approx$$
$$\approx (P-E+R)_{Pcf} \cdot \frac{1}{2} + (P-E+R)_{AI} \cdot \frac{1}{2},$$

where x are disjoint grid cells in the ocean basins, the areas of the Pcf, AI, and GO are around 177, 160, and 351 x 10^6 km^2, and the ratios 177/351 and 160/351 have been approximated by 1/2. Then, multiplying by 2 and rearranging the equation we get,

$$(P-E+R)_{Pcf} - (P-E+R)_{GO} \approx -[(P-E+R)_{AI} - (P-E+R)_{GO}].$$

Thus, wherever the signal is in the Pacific and Atlantic/Indian oceans, the anomalies with respect to the global ocean mean will always mirror each other, showing an apparent net mass exchange between them, even if such exchange does not exist.

https://doi.org/10.5194/esd-2020-54
Preprint. Discussion started: 20 July 2020


Earth System Dynamics Discussions Open Access EGU

285

Acknowledgements

We would like to thank Ben Chao for sowing the seeds of the idea of this work, during a research stay of D. García-García in Goddard Space Flight Center/NASA in 2004, and for all the subsequent fruitful discussions and advice. We thank the organizations that provide the data used in this work, which are publicly available: ERA5 data provided by the Copernicus
290 Climate Change Service Climate Data Store (CDS), https://cds.climate.copernicus.eu/cdsapp#!/home; GRACE time-variable gravity data provided by CSR, University of Texas, http://www2.csr.utexas.edu/grace; Southern Oscillation Index (SOI) from Bureau of Meteorology de Australia; Atlantic Multidecadal Oscillation (AMO) from the NOAA Earth System Research Laboratory (ESRL); Arctic Oscillation (AO) and Antarctic Oscillation (AAO) from NOAA Climate Prediction Center (CPC). This research is funded by Spanish Ministry of Science, Innovation and Universities grant number RTI2018-
295 093874-B-100.

References

Broecker, W. S., Peteet, D. M., and Rind, D.: Does the ocean-atmosphere system have more than one stable mode of operation? Nature 315, 21–26, https://doi.org/10.1038/315021a0, 1985.

300 Cessi, P., and Jones, C. S.: Warm-route versus cold-route interbasin exchange in the meridional overturning circulation. J. Phys. Oceanogr. 47, 1981–97, https://doi.org/10.1175/JPO-D-16-0249.1, 2017.

Chambers, D. P., and Willis, J. K.: Low-frequency exchange of mass between ocean basins. J. Geophys. Res. 114, C11008, https://doi.org/10.1029/2009JC005518, 2009.

305

Chao, B. F.: Caveats on the equivalent water thickness and surface mascon solutions derived from the GRACE satellite-observed time-variable gravity. Journal of Geodesy, 90, 807-813, https://doi.org/10.1007/s00190-016-0912-y, 2016.

Chen, J., Tapley, B., Seo, K.-W., Wilson, C., and Ries, J.: Improved Quantification of Global Mean Ocean Mass Change
310 Using GRACE Satellite Gravimetry Measurements. Geophys. Res. Lett. 46, 13984-13991, https://doi.org/10.1029/2019GL085519, 2019.

Cheng, M. K., and Ries, J. C.: The unexpected signal in GRACE estimates of C20. J. Geodesy 91, Issue 8, 897-91, https://doi.org/10.1007/s00190-016-0995-5, 2017.

315

https://doi.org/10.5194/esd-2020-54
Preprint. Discussion started: 20 July 2020

Colin de Verdière, A., and Ollitrault, M.: A direct determination of the World Ocean barotropic circulation. J. Phys. Oceanogr. 46, 255-273, https://doi.org/10.1175/JPO-D-15-0046.1, 2016.

Collins M., Sutherland, M., Bouwer, L., Cheong, S.-M., Frölicher, T., Jacot Des Combes, H., Koll Roxy, M., Losada, I., McInnes, K., Ratter, B., Rivera-Arriaga, E., Susanto, R. D., Swingedouw, D., and Tibig, L.: Extremes, Abrupt Changes and Managing Risk. In: IPCC Special Report on the Ocean and Cryosphere in a Changing Climate [H.-O. Pörtner, D.C. Roberts, V. Masson-Delmotte, P. Zhai, M. Tignor, E. Poloczanska, K. Mintenbeck, A. Alegría, M. Nicolai, A. Okem, J. Petzold, B. Rama, N.M. Weyer (eds.)]. In press., 2019.

Craig, P. M., Ferreira, D., and Methven, J.: The contrast between Atlantic and Pacific surface water fluxes. Tellus A: Dynamic Meteorology and Oceanography 69:1, 1330454, https://doi.org/10.1080/16000870.2017.1330454, 2017.

Czaja, A.: Atmospheric control on the thermohaline circulation. J. Phys. Oceanogr. 39, 234–247, https://doi.org/10.1175/2008JPO3897.1, 2009.

de Boer, A. M., Toggweiler, J. R., and Sigman, D. M.: Atlantic dominance of the meridional overturning circulation. J. Phys. Oceanogr. 38, 435–450, https://doi.org/10.1175/2007JPO3731.1, 2008.

de Vries, P., and Weber, S. L.: The Atlantic freshwater budget as a diagnostic for the existence of a stable shut down of the meridional overturning circulation. Geophys. Res. Lett. 32, L09606, https://doi.org/10.1029/2004GL021450, 2005.

Dijkstra, H. A.: Characterization of the multiple equilibria regime in a global ocean model. Tellus 59A, 695–705, https://doi.org/10.1111/j.1600-0870.2007.00267.x, 2007.

Dobslaw, H., Bergmann-Wolf, I., Dill, R., Poropat, L., and Flechtner, F.: Product Description Document for AOD1B Release 06. GRACE 327-750 document, Rev. 6.1, October 19, 2017.

Donohue, K. A., Tracey, K. L., Watts, D. R., Chidichimo, M. P., and Chereskin, T. K.: Mean Antarctic Circumpolar Current transport measured in Drake Passage. Geophys. Res. Lett. 43, 11760-11767, https://doi.org/10.1002/2016GL070319, 2016.

Emile-Geay, J., Cane, M. A., Naik, N., Seager, R., Clement, A. C., and van Geen, A.: Warren revisited: Atmospheric freshwater fluxes and ‘‘Why is no deep water formed in the North Pacific’’. J. Geophys. Res. 108 (C6), 3178, https://doi.org/10.1029/2001JC001058, 2003.

https://doi.org/10.5194/esd-2020-54
Preprint. Discussion started: 20 July 2020


Earth System Dynamics Discussions Open Access EGU

Ferreira, D., Cessi, P., Coxall, H. K., de Boer, A., Dijkstra, H. A., Drijfhout, S. S., Eldevik, T., Harnik, N., McManus, J. F., Marshall, D. P., Nilsson, J., Roquet, F., Schneider, T., and Wills, R. C.: Atlantic- Pacific asymmetry in deep water formation. Annual Reviews of Earth and Planetary Sciences 46, 327–352, https://doi.org/10.1146/annurev-earth-082517-010045, 2018.

Ganachaud, A., and Wunsch, C.: Improved estimates of global ocean circulation, heat transport and mixing from hydrographic data. Nature 408, 453-457, https://doi.org/10.1038/35044048, 2000.

Goosse, H., Campin, J. M., Fichefet, T., and Deleersnijder, E.: Sensitivity of a global ice-ocean model to the Bering Strait throughflow. Clim. Dyn. 13, 349 – 358, https://doi.org/10.1007/s003820050170, 1997.

Gordon, A. L.: Interocean exchange of thermocline water, J. Geophys. Res. 91, 5037–5046, https://doi.org/10.1029/JC091iC04p05037, 1986.

Hartmann, D. L. Global Physical Climatology. International Geophysics v. 56 (Academic Press, 1994).

Hersbach, H., de Rosnay, P., Bell, B., Schepers, D., Simmons, A., Soci, C., Abdalla, S., Alonso-Balmaseda, M., Balsamo, G., Bechtold, P., Berrisford, P., Bidlot, J.-R., de Boisséson, E., Bonavita, M., Browne, P., Buizza, R., Dahlgren, P., Dee, D., Dragani, R., Diamantakis, M., Flemming, J., Forbes, R., Geer, A. J., Haiden, T., Hólm, E., Haimberger, L., Hogan, R., Horányi, A., Janiskova, M., Laloyaux, P., Lopez, P., Munoz-Sabater, J., Peubey, C., Radu, R., Richardson, D., Thépaut, J.-N., Vitart, F., Yang, X., Zsótér, E., and Zuo, H..: Operational global reanalysis: progress, future directions and synergies with NWP. ERA Report Series 27, doi: 10.21957/tkic6g3wm, 2018.

Jones, C. S., and Cessi, P. Size Matters: Another Reason Why the Atlantic Is Saltier than the Pacific. J. Phys. Oceanogr. 47, 2843-2859, https://doi.org/10.1175/JPO-D-17-0075.1, 2017.

Lagerloef, G., Colomb, F. R., Le Vine, D., Wentz, F., Yueh, S., Ruf, C., Lilly, J., Gunn, J., Chao, Y., deCharon, A., Feldman, G., and Swift, C.: The Aquarius/SAC-D Mission: Designed to meet the salinity remote-sensing challenge. Oceanography 21 (1), 68-81, https://doi.org/10.5670/oceanog.2008.68, 2008.

Lorenz, C., Kunstmann, H., Devaraju, B., Tourian, M. J., Sneeuw, N., and Riegger, J.: Large-Scale Runoff from Landmasses: A Global Assessment of the Closure of the Hydrological and Atmospheric Water Balances. J. Hydrometeor. 15, 2111-2139, https://doi.org/10.1175/JHM-D-13-0157.1, 2014.

https://doi.org/10.5194/esd-2020-54
Preprint. Discussion started: 20 July 2020

Marsh, R., Hazeleger, W., Yool, A., and Rohling, E. J.: Stability of the thermohaline circulation under millennial CO2 forcing and two alternative controls on Atlantic salinity. Geophys. Res. Lett. 34, L03605, https://doi.org/10.1029/2006GL027815, 2007.

Newsom, E. R., and Thompson, A. F.: Reassessing the role of the Indo-Pacific in the ocean's global overturning circulation. Geophys. Res. Lett. 45, 12422–12431, https://doi.org/10.1029/2018GL080350, 2018.

Nilsson, J., Langen, P. L., Ferreira, D., and Marshall, J.: Ocean basin geometry and the salinification of the Atlantic Ocean. J. Clim. 26, 6163–6184, https://doi.org/10.1175/JCLI-D-12-00358.1, 2013

Nilsson, T., and Elgered, G.: Long-term trends in the atmospheric water vapor content estimated from ground-based GPS data. J. Geophys. Res. 113, D19101, https://doi.org/10.1029/2008JD010110, 2008.

Oki, T., and Sud, Y. C.: Design of Total Runoff Integrating Pathways (TRIP) - A Global River Channel Network. Earth Interactions 2, Paper No. 1, https://doi.org/10.1175/1087-3562(1998)002<0001:DOTRIP>2.3.CO;2, 1998.

Patton, A., Politis, D. N, and White, H.: Correction to "Automatic Block-Length Selection for the Dependent Bootstrap", Econometric Reviews 28, 372-375, https://doi.org/10.1080/07474930802459016, 2009.

Peltier, W. R., Argus, D. F., and Drummond, R.: Comment on "An assessment of the ICE-6G_C (VM5a) glacial isostatic adjustment model" by Purcell et al. J. Geophys. Res. Solid Earth 123, 2019– 2028, https://doi.org/10.1002/2016JB013844, 2018.

Politis, D. N. & Romano, J. P.: The stationary bootstrap. J. Amer. Statist. Assoc. 89, 1303-1313. https://doi.org/10.1080/01621459.1994.10476870, 1994.

Rahmstorf, S. On the freshwater forcing and transport of the Atlantic thermohaline circulation. Clim. Dyn. 12, 799–811, https://doi.org/10.1007/s003820050144, 1996.

Reason, C. J. C., and Power, S. B.: The influence of the Bering Strait on the circulation in a coarse resolution global ocean model. Clim. Dyn. 9, 363–369, https://doi.org/10.1007/BF00223448, 1994.

Reid, J. L.: On the temperature, salinity, and density differences between the Atlantic and Pacific oceans in the upper kilometre. Deep Sea Research 7, Issue 4, 265-275, https://doi.org/10.1016/0146-6313(61)90044-2, 1953.

Reul, N., Fournier, S., Boutin, J., Hernandez, O., Maes, C., Chapron, B., Alory, G., Quilfen, Y., Tenerelli, J., Morisset, S., Kerr, Y., Mecklenburg, S., and Delwart, S.: Sea Surface Salinity Observations from Space with the SMOS Satellite: A New Means to Monitor the Marine Branch of the Water Cycle. Surv. Geophys. 35, 681-722, https://doi.org/10.1007/s10712-013-9244-0, 2014.

Rodell, M., Beaudoing, H. K., L'Ecuyer, T. S., Olson, W. S., Famiglietti, J. S., Houser, P. R., Adler, R., Bosilovich, M. G., Clayson, C. A., Chambers, D., Clark, E., Fetzer, E. J., Gao, X., Gu, G., Hilburn, K., Huffman, G. J., Lettenmaier, D. P., Liu, W. T., Robertson, F. R., Schlosser, C. A., Sheffield, J., and Wood, E. F.: The Observed State of the Water Cycle in the Early Twenty-First Century, J. Climate 28, 8289-8318, https://doi.org/10.1175/JCLI-D-14-00555.1, 2015.

Ropelewski, C. F., and Halpert, M. S.: Global and regional precipitation patterns associated with El Niño-Southern Oscillation. Mon. Weather Rev. 115, 1606-1625, https://doi.org/10.1175/1520-0493(1987)115<1606:GARSPP>2.0.CO;2, 1987.

Save, H., Bettadpur, S., and Tapley, B. D.: High resolution CSR GRACE RL05 mascons. J. Geophys. Res. Solid Earth 121, https://doi.org/10.1002/2016JB013007, 2016.

Save, H.: "CSR GRACE RL06 Mascon Solutions", https://doi.org/10.18738/T8/UN91VR, Texas Data Repository Dataverse, V1, https://doi.org/10.18738/T8/UN91VR, 2019.

Swenson, S., Chambers, D., and Wahr, J.: Estimating geocenter variations from a combination of GRACE and ocean model output, J. Geophys. Res., 113, B08410, https://doi.org/10.1029/2007JB005338, 2008.

Tapley, B. D., Bettadpur, S., Watkins, M. & Reigber, C. The Gravity Recovery and Climate Experiment: Mission overview and early results. Geophys. Res. Lett. 31, L09607, https://doi.org/10.1029/2004GL019920, 2004.

Tapley, B. D., Watkins, M. M., Flechtner, F., Reigber, C., Bettadpur, S., Rodell, M., Sasgen, I., Famiglietti, J. S., Landerer, F. W., Chambers, D. P., Reager, J. T., Gardner, A. S., Save, H., Ivins, E. R., Swenson, S. C., Boening, C., Dahle, C., Wiese, D. N., Dobslaw, H., Tamisiea, M. E., and Velicogna, I.: Contributions of GRACE to understanding climate change. Nat. Clim. Change 9, 358-369, https://doi.org/10.1038/s41558-019-0456-2, 2019.

Vellinga, M., and Wood, R. A.: Global climate impacts of a collapse of the Atlantic thermohaline circulation. Clim. Change 54, 251–267, https://doi.org/10.1023/A:1016168827653, 2002.

https://doi.org/10.5194/esd-2020-54
Preprint. Discussion started: 20 July 2020

Vigo, M. I., García-Garcia, D., Sempere, M. D., and Chao, B. F.: 3D Geostrophy and Volume Transport in the Southern Ocean. Remote Sens. 10, 715, https://doi.org/10.3390/rs10050715, 2018.

Wadley, M. R., and Bigg, G. R.: Impact of flow through the Canadian Archipelago and Bering Strait on the North Atlantic and Arctic circulation: An ocean modelling study. Q. J. R. Meteorol. Soc. 128, 2187 – 2203, https://doi.org/10.1256/qj.00.35, 2002.

Warren, B. A.: Deep circulation of the World Ocean. In: Warren, B.A., Wunsch, C. (eds) Evolution of physical oceanography. MIT Press, Cambridge, Ma., USA, https://doi.org/10.4319/lo.1982.27.2.0397a, 1981.

Warren, B. A.: Why is no deep water formed in the North Pacific? J. Mar. Res. 41, 327-347, https://doi.org/10.1357/002224083788520207, 1983.

Willis, J. K., Chambers, D. P., and Nerem, R. S.: Assessing the globally averaged sea level budget on seasonal to interannual time-scales. J. Geophys. Res. 113, C06015, https://doi.org/10.1029/2007JC004517, 2008.

Woodgate, R. A., Weingartner, T. J., and Lindsay, R.: Observed increases in Bering Strait oceanic fluxes from the Pacific to the Arctic from 2001 to 2011 and their impacts on the Arctic Ocean water column. Geophys. Res. Lett. 39, L24603, https://doi.org/10.1029/2012GL054092, 2012.

Wouters, B., Bonin, J. A., Chambers, D. P., Riva, R. E. M., Sasgen, I., Wahr, J.: GRACE, time-varying gravity, Earth system dynamics and climate change. Rep. Prog. Phys. 77, 116801, doi:10.1088/0034-4885/77/11/116801, 2014.

Zaucker, F., Stocker, T. F. & Broecker, W. S. Atmospheric freshwater fluxes and their effect on the global thermohaline circulation. J. Geophys. Res. 99, 12443–12457, https://doi.org/10.1029/94JC00526, 1994.

https://doi.org/10.5194/esd-2020-54
Preprint. Discussion started: 20 July 2020

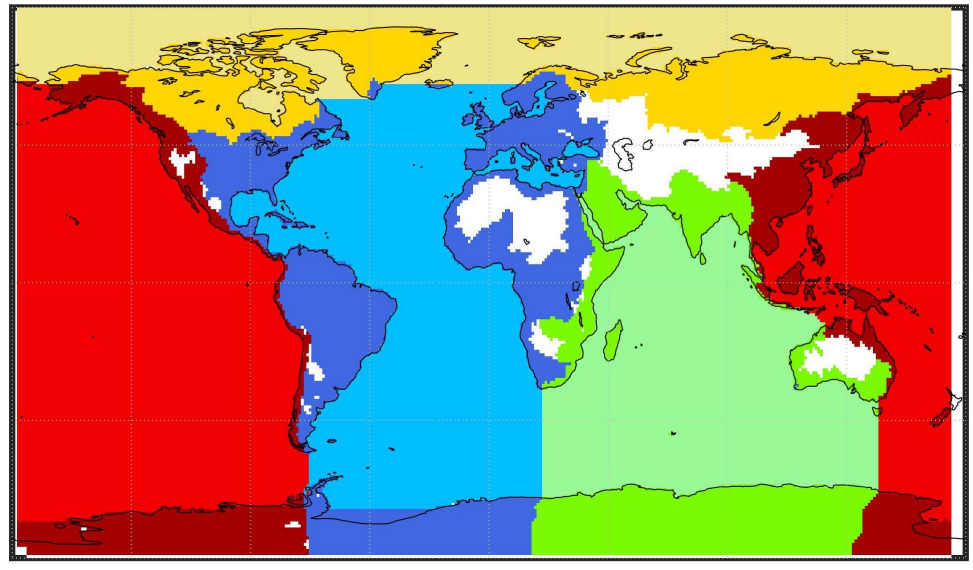

Figure 1. Pacific, Atlantic, Indian, and Arctic Ocean basins and their associated continental drainage basins (white represent endorheic basins).

https://doi.org/10.5194/esd-2020-54
Preprint. Discussion started: 20 July 2020

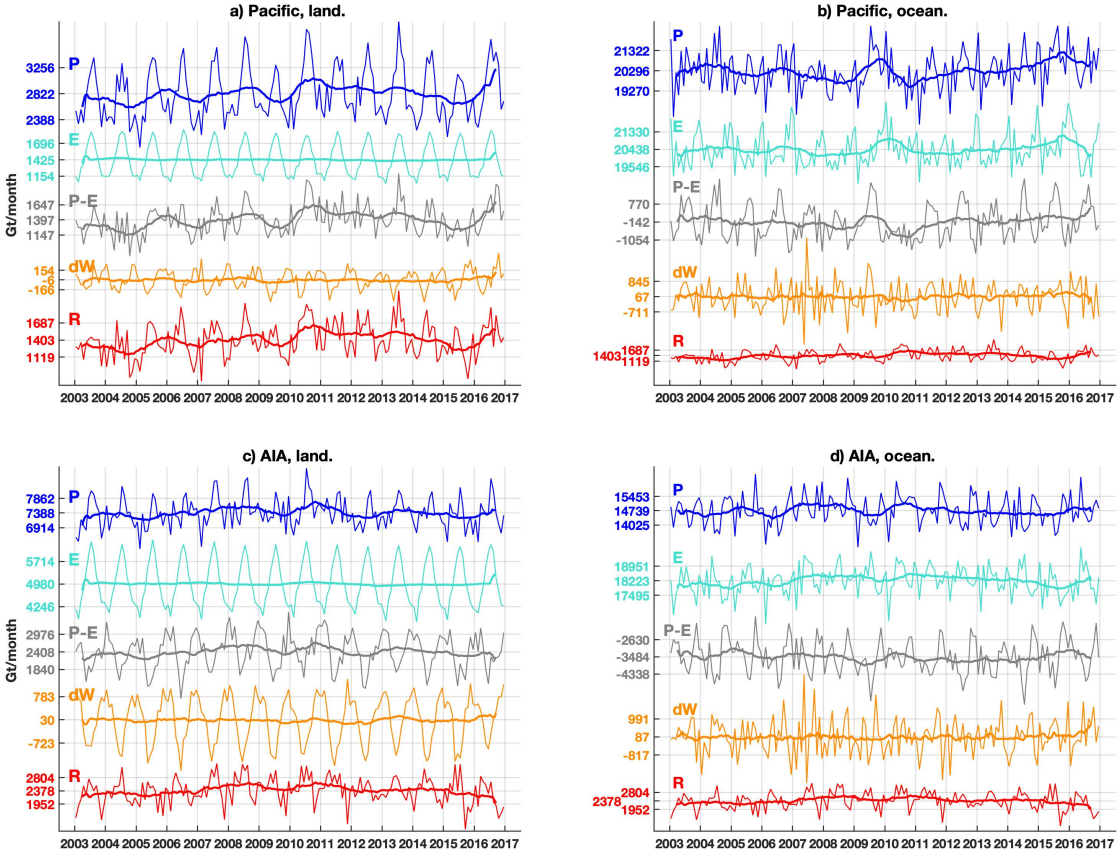

Figure 2. WT of Equations (1) and (2) in the Pacific (first row), Atlantic/Indian/Arctic (AIA) oceans collectively (second row), and their drainage basins. First column: associated land drainage basins; second column: ocean basins. Labels in the vertical axis correspond to the mean ± standard deviation of the associated curve. Thick lines are 12-month running means. All 5 curves in the same panel plotted on the same scale.

https://doi.org/10.5194/esd-2020-54
Preprint. Discussion started: 20 July 2020

Earth System Dynamics
Discussions
Open Access
EGU

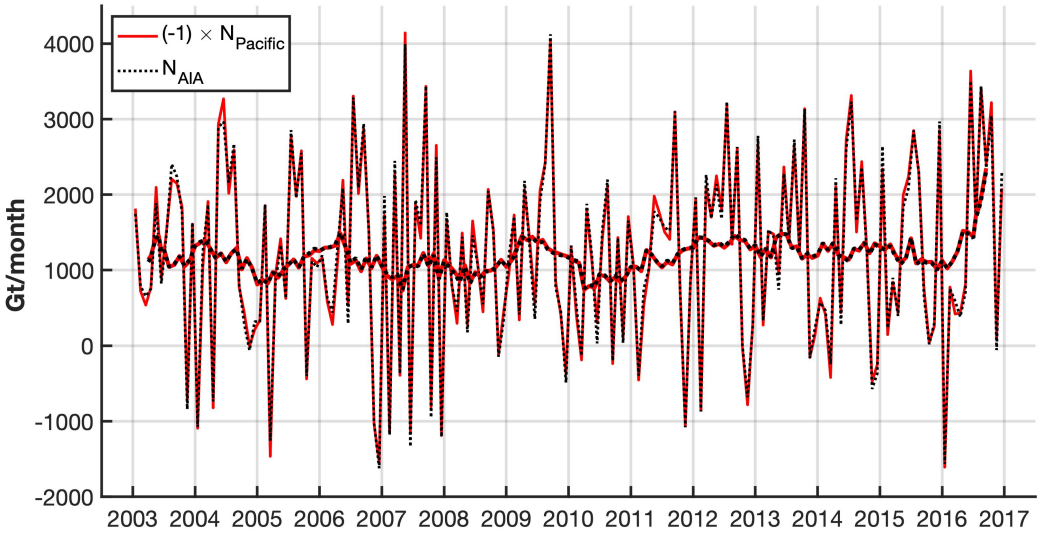

495

Figure 3. Monthly time series of WT flux from the Pacific to the AIA Oceans. Red curve is (the opposite of) the Pacific outflow, and black curve if the AIA inflow. Thick lines are their 12-month running means.

https://doi.org/10.5194/esd-2020-54
Preprint. Discussion started: 20 July 2020

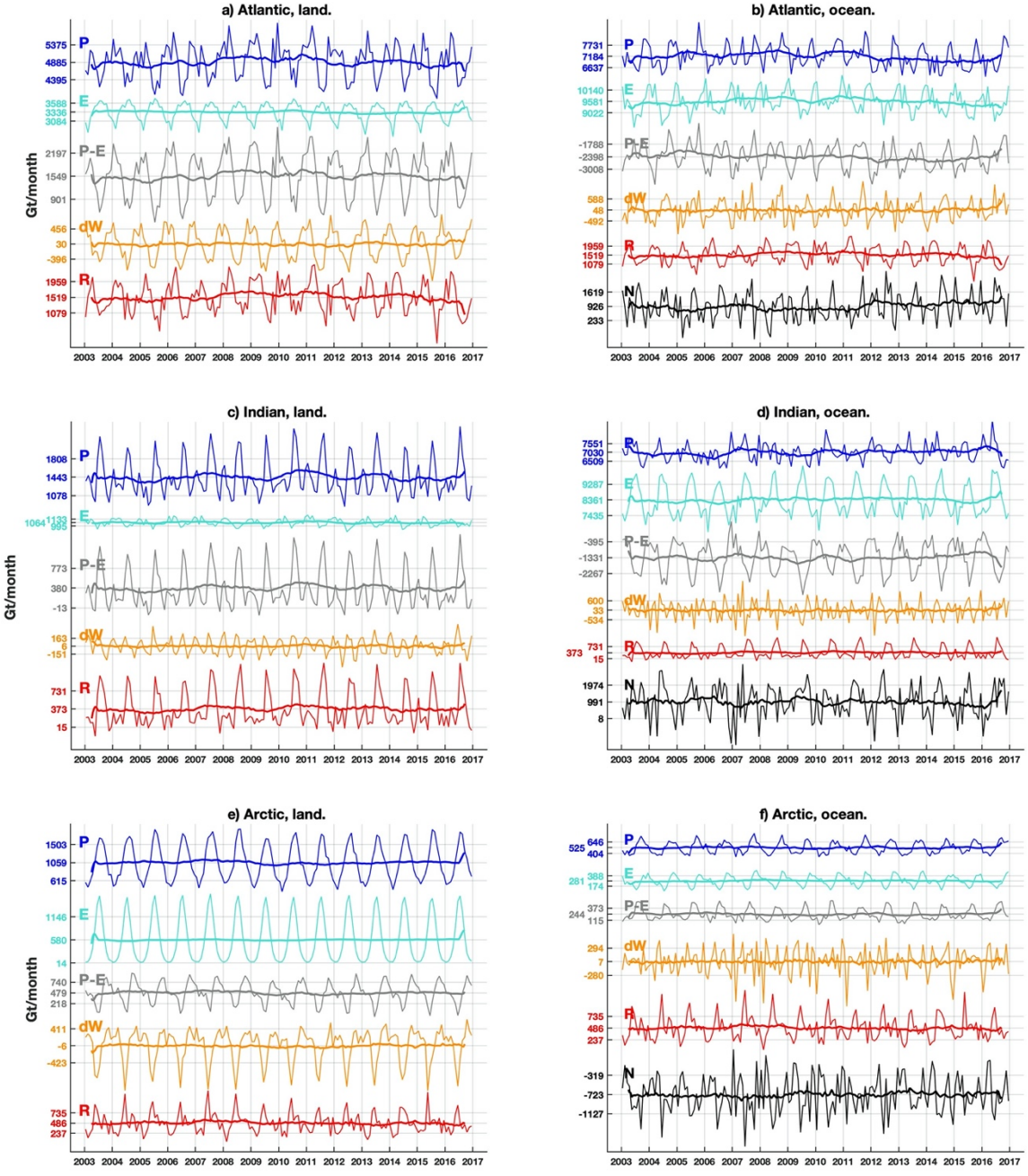

Figure 4. As Figure 2 but for Atlantic, Indian, and Arctic Oceans. Black lines are the WT N component.

https://doi.org/10.5194/esd-2020-54
Preprint. Discussion started: 20 July 2020

Earth System Dynamics
Discussions
Open Access
EGU

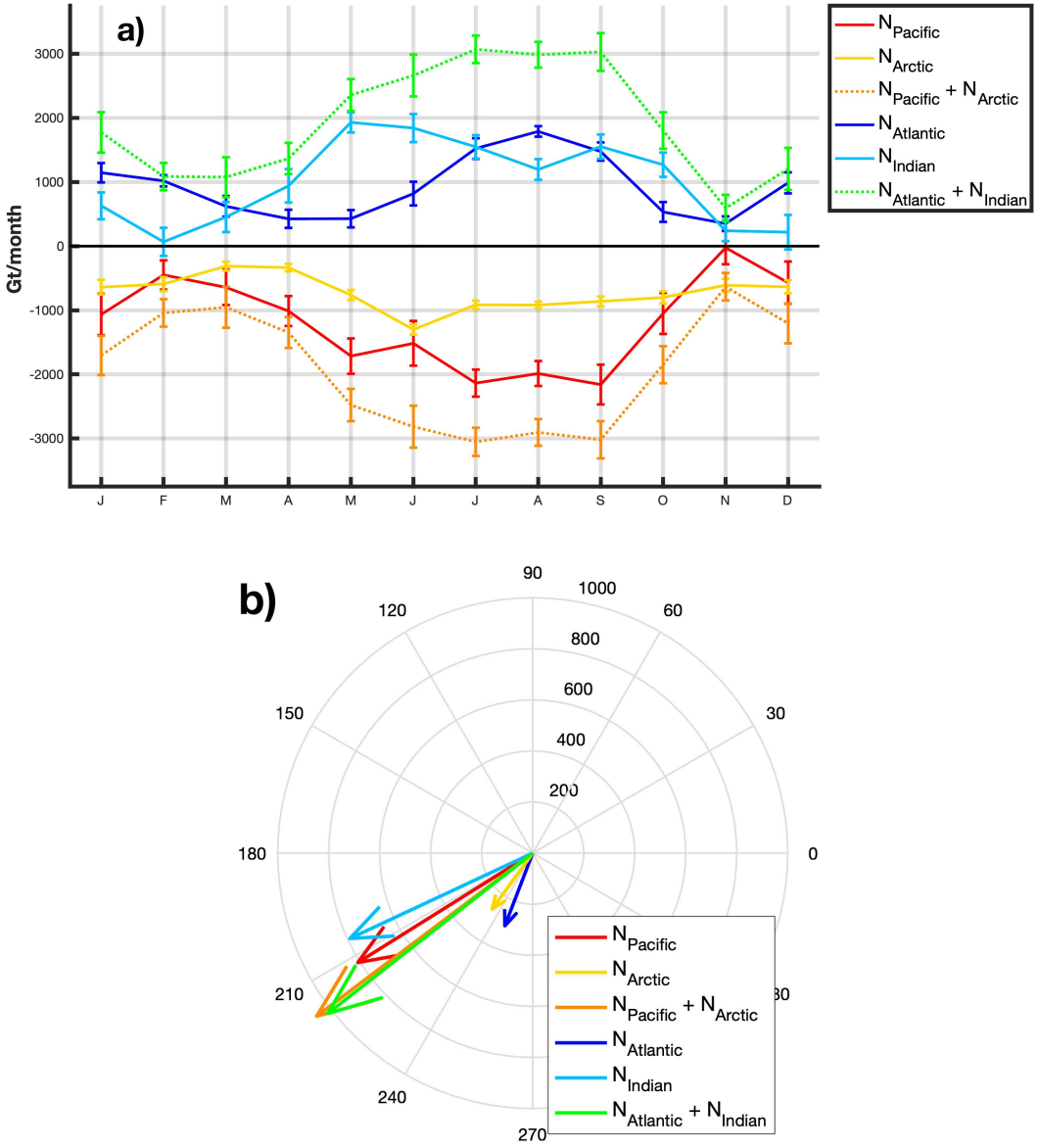

505

Figure 5. (a) Annual climatology time series (error bar is one standard deviation), and (b) phasor diagram (amplitude in unit of Gt/month, phase angle according to Equation 3) of the inflow/outflow WT of the ocean basins.

https://doi.org/10.5194/esd-2020-54
Preprint. Discussion started: 20 July 2020

Earth System Dynamics
Discussions
Open Access
EGU

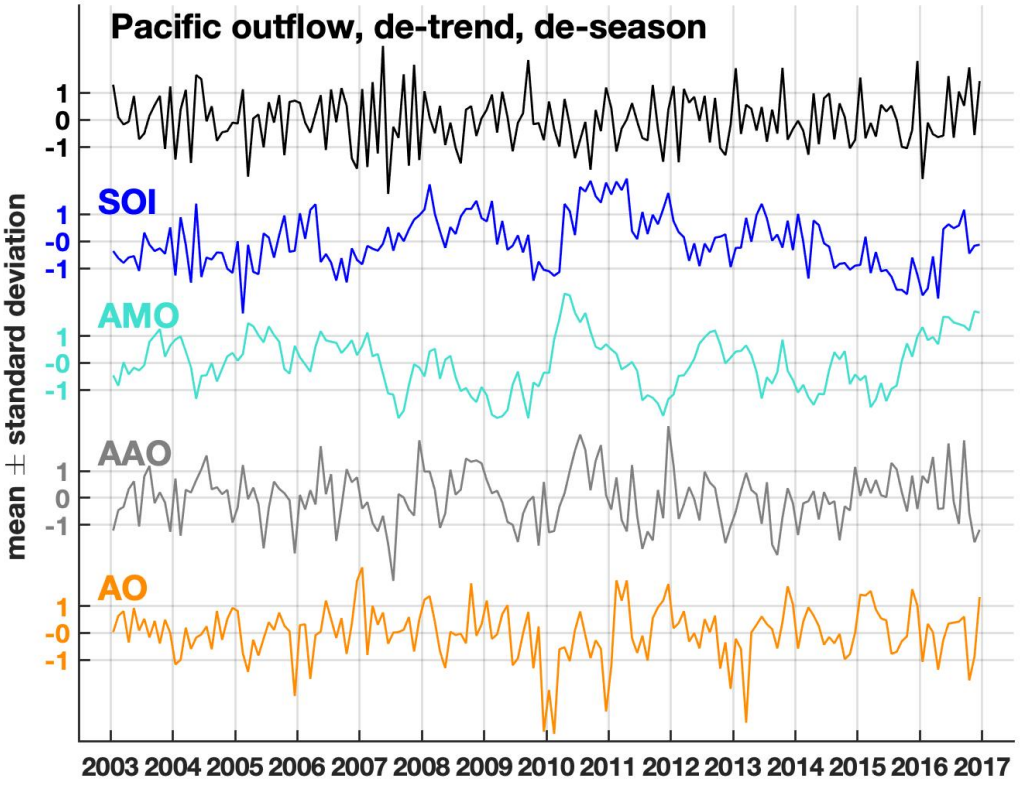

510 **Figure 6. Pacific outflow and climatic indices for ENSO, AMO, AO, and AAO.** Time series of Pacific outflow is de-trend and de-season. All time series are normalized to one standard deviation.

https://doi.org/10.5194/esd-2020-54
Preprint. Discussion started: 20 July 2020

Earth System Dynamics Discussions
Open Access
EGU

515 **Table 1. Mean and annual signals of the net WT for different ocean basins according to Equation (3) .**

		Mean (CI_{95})	Annual signal (CI95)		
		(Gt/month)	Amplitude (Gt/month)	Phase (degree)	Peak date
Outflows	Pacific	1194 (1087, 1308)	809 (637, 975)	212 (200, 224)	August 3rd
	Arctic	723 (709, 738)	271 (242, 302)	234 (228, 240)	August 25th
	Pacific + Arctic	1917 (1826, 2010)	1061 (904, 1216)	217 (209, 225)	August 8th
Inflows	AIA	1194 (1086, 1304)	767 (610, 926)	212 (199, 224)	August 3rd
	Atlantic	926 (863, 991)	305 (219, 384)	249 (234, 266)	September 9th
	Indian	991 (911, 1067)	791 (664, 918)	205 (196, 214)	July 27th
	Atlantic + Indian	1917 (1821, 2015)	1020 (876, 1172)	218 (209, 226)	August 9th